Toxicology 500 (2023) 153682

Contents lists available at ScienceDirect

Toxicology

journal homepage: www.elsevier.com/locate/toxicol

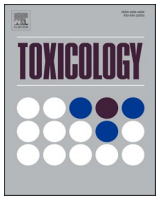

The variability in CYP3A4 activity determines the metabolic kinetic characteristics of ketamine

Mengfang Li [a,1], Qingqing Li [b,1], Dan Lin [c], Xiang Zheng [b], Lehao Jin [b], Jianping Cai [d,*], Guoxin Hu [b,c,**], Jianchang Qian [b,*]

[a] Department of Emergency Medicine, The First Affiliated Hospital of Wenzhou Medical University, Wenzhou, Zhejiang, China
[b] Institute of Molecular Toxicology and Pharmacology, School of Pharmaceutical Sciences, Wenzhou Medical University, Wenzhou, Zhejiang, China
[c] Wenzhou Medical University Forensic Center, Wenzhou, Zhejiang, China
[d] The Key Laboratory of Geriatrics, Beijing Hospital & Beijing Institute of Geriatrics, Ministry of Health, Beijing, China

ARTICLE INFO

Handling Editor: Dr. Mathieu Vinken

Keywords:
Ketamine
CYP3A4
Gene polymorphism
Kinetics
Voriconazole

ABSTRACT

Ketamine is a psychotropic drug that can cause significant neurological symptoms and is closely linked to the activity of the CYP3A4 enzyme. This study aimed to examine the diversity of CYP3A4 activity affects the metabolism of ketamine, focusing on genetic variation and drug-induced inhibition. We used a baculovirus-insect cell expression system to prepare recombinant human CYP3A4 microsomes. Then, in vitro enzyme incubation systems were established and used UPLC-MS/MS to detect ketamine metabolite. In rats, we investigated the metabolism of ketamine and its metabolite in the presence of the CYP3A4 inhibitor voriconazole. Molecular docking was used to explore the molecular mechanism of inhibition. The results showed that the catalytic activity of CYP3A4.5, .17, .23, .28, and .29 significantly decreased compared to CYP3A4.1, with a minimum decrease of 3.13%. Meanwhile, the clearance rate of CYP3A4.2, .32, and .34 enhanced remarkably, ranging from 40.63% to 87.50%. Additionally, hepatic microsome incubation experiments revealed that the half-maximal inhibitory concentration (IC_{50}) of voriconazole for ketamine in rat and human liver microsomes were 18.01 ± 1.20 μM and 14.34 ± 1.70 μM, respectively. When voriconazole and ketamine were co-administered, the blood exposure of ketamine and norketamine significantly increased in rats, as indicated by the area under the concentration-time curve (AUC) and maximum concentration (C_{max}). The elimination half-life ($t_{1/2Z}$) of these substances was also prolonged. Moreover, the clearance ($CL_{z/F}$) of ketamine decreased, while the apparent volume of distribution ($V_{z/F}$) increased significantly. This might be attributed to the competition between voriconazole and ketamine for binding sites on the CYP3A4 enzyme. In conclusion, variations in CYP3A4 activity would result in the stratification of ketamine blood exposure.

Abbreviations: ACN, acetonitrile; ALA, alanine; ANOVE, analysis of variance; ARG, arginine; ASP, aspartic acid; ARRIVE, Animal Research: Reporting of In Vivo Experiments; AUC, area under the concentration-time curve; CL_{int}, intrinsic clearance; $CL_{z/F}$, blood clearance; C_{max}, maximum blood concentration; CMC-Na, carboxymethylcellulose sodium salt; CYP450, cytochrome P450; CYS, cysteine; DAS, Drug and statistics; DDIs, drug-drug interactions; HIS, histidine; HLM, human liver microsomes; IC_{50};, half-maximal inhibitory concentration; ILE, isoleucine; IS, internal standard; GLN, glutamine; K_m, Michaelis-Menten constant; LEU, leucine; LLOQ, lower limit of quantification; MDL, midazolam; MET, methionine; ME, matrix effect; MRM, multiple reaction monitoring; NADPH, reduced nicotinamide adenine dinucleotide phosphate; ND, not determined; NMDA, N-methyl-D-aspartate; PHE, phenylalanine; PRO, proline; QC, quality control; RLM, rat liver microsomes; SD, standard deviation; SD rats, Sprague-Dawley rats; SER, serine; $t_{1/2z}$, elimination half time; THR, threonine; T_{max}, peak time; TRP, tryptophane; VAL, valine; $V_{max,}$;, maximum velocity of the reaction; $V_{z/F}$, apparent volume of distribution; UPLC-MS/MS, ultra-performance liquid chromatography-tandem mass spectrometry.

* Corresponding authors.
** Corresponding author at: Institute of Molecular Toxicology and Pharmacology, School of Pharmaceutical Sciences, Wenzhou Medical University, Wenzhou, Zhejiang, China.
E-mail addresses: caijp61@vip.sina.com (J. Cai), hgx@wmu.edu.cn (G. Hu), qianjc@wmu.edu.cn (J. Qian).
[1] These authors contribute equally to the work

https://doi.org/10.1016/j.tox.2023.153682
Received 28 September 2023; Received in revised form 16 November 2023; Accepted 21 November 2023
Available online 24 November 2023

1. Introduction

Ketamine, a derivative of phenylcyclidine, has been used as a clinical anesthetic since the 1960 s for patients and has also demonstrated lower occurrence rates of emergence delirium (Culp et al. 2020). Compared to other inhalation anesthetics, ketamine is considered safer as it maintains breathing and hemodynamic stability (Dong et al. 2015). Recent research has shown that ketamine has additional pharmacological effects including anti-inflammatory, antidepressant, and sedative properties through its antagonistic effects on N-methyl-D-aspartate (NMDA) receptors (Gorlin et al. 2016; Hashimoto, 2009; Reus et al. 2017). However, irregular use of ketamine can lead to hallucinogenic effects, cognitive disorders, mental dependence, and other side effects (Zanos et al. 2018). The severity of these adverse reactions is dose-dependent, with poisoning, hallucinations, and even sudden death (Licata et al. 1994). Variations in ketamine metabolism have been attributed to differences in cytochrome P450 (CYP450) enzyme expression, which is an important factor in determining therapeutic efficacy (Cheng et al. 2007; Desta et al. 2012; Hijazi and Boulieu, 2002).

CYP450 is a crucial enzyme involved in the phase I of liver biotransformation, responsible for metabolizing 95% of organic chemicals (Almazroo et al. 2017; Guengerich et al. 2016). When it comes to ketamine, it is mainly converted into norketamine in the liver by two specific enzymes, CYP3A4 and CYP2C9. Among them, CYP3A4 plays a predominant role (Hijazi and Boulieu, 2002; Zheng et al. 2017). It's located at 7q22.1 on chromosome 7 and possesses abundant genetic polymorphic loci (Spurr et al. 1989). The functional differences in the CYP3A4 enzyme caused by these polymorphic loci are important contributing factors to individual variations in substrate drug concentrations (Nicolas et al. 2009; Roco et al. 2012; Werk and Cascorbi, 2014). Hence, establishing the association between CYP3A4 genotype and metabolic phenotype is useful for tailoring ketamine administration.

The co-administration of drugs can also alter the activity of the CYP3A4 enzyme through inhibition or induction. Previous research has demonstrated that ketoconazole, a specific inhibitor of CYP3A4, reduced the N-demethylation of ketamine by approximately 40% (Hijazi and Boulieu, 2002). Additionally, rifampin, a well-known inducer of CYP3A4, decreased the area under the concentration-time curve of ketamine by 10% and norketamine by 50% (Noppers et al. 2011). This interference can lead to various outcomes, such as enhanced therapeutic effects, increased risk of toxic side effects, or even treatment failure.

In this study, we investigated the impact of genetic factors and drug-induced inhibition of CYP3A4 activity on the metabolism of ketamine using in vitro and in vivo approaches. The results will provide fundamental data for personalized application and monitoring of ketamine.

2. Materials and methods

2.1. Chemicals and materials

Ketamine and norketamine were purchased from Sigma-Aldrich (Washington, DC, USA). Voriconazole was bought from J&K Scientific (Shanghai, China). Midazolam (MDL) was obtained from the second affiliated hospital of Wenzhou Medical University (Wenzhou, China). Reduced nicotinamide adenine dinucleotide phosphate (NADPH) was procured from Roche Pharmaceutical Ltd. (Basel, Switzerland). Rat liver microsomes (RLM) and human liver microsomes (HLM) were from Corning Life Sciences Co., Ltd (NY, USA). In the current study, all solvents and reagents were of analytical grade.

2.2. Preparation of recombinant human CYP3A4 and cytochrome b5 baculosomes

Preparation and quality control methods for recombinant human CYP3A4 microsomes can be referred to our team's previous reports (Fang et al. 2017). The 22 CYP3A4 variants were cloned together with cytochrome P450 oxidoreductase (CYPOR) into the dual expression vector pFastbac™ Dual (ThermoFisher, Waltham, Massachusetts), and confirmed by sequencing. The plasmids were transformed into DH10Bac competent cells, and recombinant bacmid DNA was obtained through blue-white screening and PCR. The bacmid DNA was transfected into sf21 cells using Cellfectin™ II (ThermoFisher, Waltham, Massachusetts). The cells expressing high levels of CYP3A4 and CYPOR were obtained following the instructions of the Bac-to-Bac™ baculovirus expression system. Subsequently, the cells were sonicated and microsomes were prepared and obtained using ultracentrifugation. The protein expression levels of the target proteins were examined using protein immunoblotting, and the quantification of CYP was performed using carbon monoxide difference spectrophotometry [formula: C (nmol/ml) = (OD450nm-OD490nm) × 1000/91]. Cytochrome b5 baculosomes was obtained as the same as illustrated above.

Table 1
Mass transitions and key operational characteristics of the analytes.

Analytes	Mass transition (*m/z* to *m/z*)	Cone (V)	Collision (V)
Ketamine	237.96 → 125.00	30	18
Norketamine	224.00 → 207.00	25	10
Midazolam (IS)	326.10 → 291.00	60	30

2.3. Conditions of UPLC-MS/MS

To analyze qualitative analytes, the H-Class/Xevo TQ-Smicro was equipped with UPLC-MS/MS. The multiple reaction monitoring (MRM) method was used, with the ion mode set to ES^+. Table 1 provided the mass transitions and key operational characteristics of the detected substances. Analytes were separated using a UPLC BEH C18 column (2.1 × 50 mm, 1.7 μM; Waters, USA), with the column or automatic sampler temperature set at 35 ℃ or 4 ℃, respectively. The mobile phase consisted of 0.1% formic acid (A) and acetonitrile (B), with an elution rate of 0.3 ml/min for 2.5 min. The desolvation temperature was optimized at 500 ℃.

2.4. Enzymatic incubation system

The incubation system was prepared with a total volume of 200 μL, containing 5 pmoL recombinant human CYP3A baculosomes, 5 pmoL cytochrome b5, 2.74 μL ketamine (100 μM), 10 μL NADPH (20 mM) and 177.26 μL Tris-HCl (100 mM, pH 7.4). Amount of CYP3A4 and b5 baculosomes added was optimized to achieve a linear relationship with the rate of product formation. The mixture was pre-incubated at 37 ℃ for 5 min. Then, NADPH was added to initiate the reaction. 40 min later, the mixture was freezing at − 80 ℃. After approximately 15 min, 400 μL of acetonitrile (ACN) and 40 μL of midazolam (500 ng / ml) were added to precipitate protein and serve as the internal standard (IS), respectively. The sample was then vortexed for 2 min and centrifuged at 13,000 rpm for 10 min. Finally, 20 μL of supernatant was mixed with 180 μL of ultra-pure water for UPLC-MS/MS detection. To determine the intrinsic clearance (CL_{int}) of CYP3A4, the concentration of ketamine varied from 20 to 1000 μM. The software GraphPad Prism 9.5 was used for non-linear regression analysis to abtaine the values of K_m and V_{max}. CL_{int} was calculated by dividing V_{max} by K_m.

For the evaluation of voriconazole's effect on ketamine metabolism in vitro, the incubation system consisted of 0.2 mg/ml RLM or HLM, voriconazole (0, 0.01, 0.1, 1, 10, and 100 μM), 2.74 μL ketamine (100 μM, based on K_m value), 10 μL NADPH (20 mM) and 177.26 μL Tris-HCl (100 mM, pH 7.4) to a total volume of 200 μL. The subsequent processing steps were consistent as described above.

2.5. Animal experiment

5–8 week-old healthy Sprague-Dawley male rats were obtained from

Fig. 1. CYP3A4 and CYP2C9 catalyze the metabolism of ketamine to produce norketamine.

Beijing Vital River Laboratory Animal Technology Co., Ltd. (Beijing, China). After an adaptation period of 1–2 weeks at the Experimental Animal Center of Wenzhou Medical University, start the experiments when the rats reach a weight of 250 ± 10 g. All animal experiments were carried out in accordance with the National Research Council's Guide for the Care and Use of Laboratory Animals. The study protocol was approved by the Experimental Animal Ethics Committee of Wenzhou Medical University (ID Number: wydw2023–0461), and reported in accordance with the ARRIVE guidelines (Percie du Sert et al. 2020).

Ten male Sprague-Dawley rats were randomly allocated into two groups: a single group receiving 1.5 mg/kg ketamine (sublingual vein, i.v.) and a combined group receiving 30 mg/kg voriconazole (p.o.) (Lelievre et al. 2018) and 1.5 mg/kg ketamine (i.v.) (Sleigh et al. 2019). Prior to the experiment in order to eliminate the influence of food on drug absorption, the rats were fasted for 12 h, with access to water only. In the combined group, 30 mg/kg voriconazole was administered orally, while the single group received the corresponding solvent (0.5% carboxymethylcellulose sodium salt). Both groups were then anesthetized with isoflurane. After 30 min, a dose of 1.5 mg/kg ketamine was administered intravenously. Blood samples were collected from the tail vein at 0.0167, 0.0833, 0.25, 0.5, 0.75, 1, 2, 3, 4, 6, 8, and 12 h after administration, with a volume of 200 μL each time. After each blood collection, hemostasis was performed. Four hours after administration of ketamine, the rats were provided with food and allowed free access to water. During the experimental process, no abnormal conditions were observed in the rats. The blood samples were collected in heparin-treated tubes and centrifuged at 8000 rpm for 10 min. For plasma sample preparation, 100 μL of plasma was mixed with 200 μL of acetonitrile and 20 μL of MDL (100 ng/ml). After thorough vortexing and centrifugation, 50 μL of the supernatant was mixed with 150 μL of ultra-pure water for further analysis.

2.6. Molecular docking

Autodock vina software was used to conduct molecular docking. Initially, ChemBioDraw Ultra 14.0 software was employed to map the structure of ketamine and voriconazole. These structures were then converted into a 3D format and subjected to energy optimization using the MMFF94 force field. AutodockTools 1.5.6 was utilized to merge non-polar hydrogen and define rotation bonds before converting the

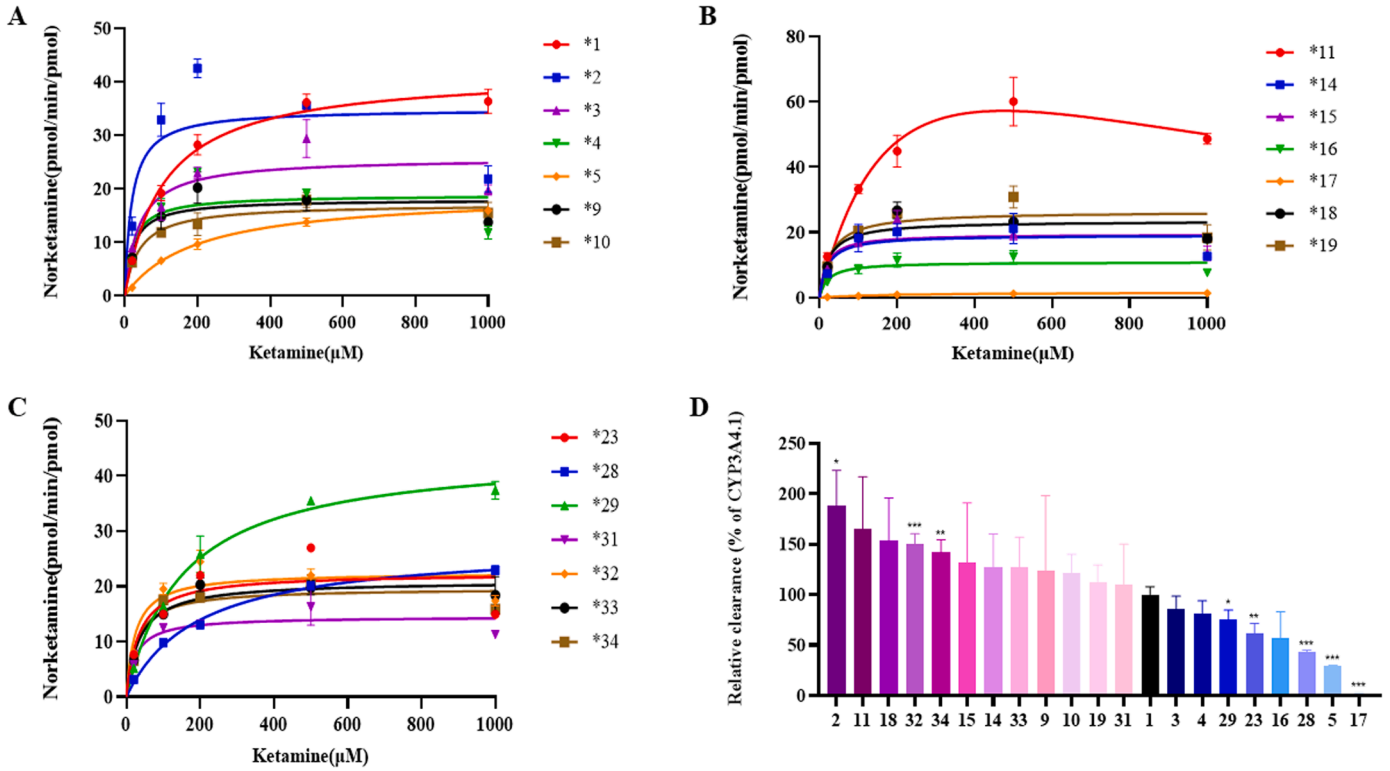

Fig. 2. Enzyme kinetics curve for CYP3A4 metabolism of ketamine. The kinetics assay was performed as indicated in the method. (A-C) Michaelis-Menten curves of CYP3A4 variants in metabolizing ketamine. (D) Relative clearance of ketamine metabolized by CYP3A4 variants compared to CYP3A4.1. Values are expressed as mean ± SD, n = 3. CYP3A4 variants vs CYP3A4.1. * $P < 0.05$, * * $P < 0.01$, * ** $P < 0.001$.

Table 2
Kinetic parameters for ketamine metabolic enzyme activity of 21 CYP3A4 variants compared with CYP3A4.1.

Variants	V_{max} (pmol/min per pmol of CYP3A4)	K_m (μM)	CL_{int} (V_{max}/K_m) (μL/min/mmol P450)
CYP3A4.1	53.57 ± 1.71	169.60 ± 9.10	0.32 ± 0.03
CYP3A4.2	132.11 ± 61.47	241.60 ± 164.88	0.60 ± 0.11 * ↑
CYP3A4.3	68.19 ± 33.16	269.40 ± 176.38	0.27 ± 0.04
CYP3A4.4	96.80 ± 34.01	385.33 ± 161.29	0.26 ± 0.04
CYP3A4.5	20.87 ± 2.95 * ** ↓	227.83 ± 38.57	0.09 ± 0.00 * ** ↓
CYP3A4.9	51.80 ± 36.06	216.54 ± 244.78	0.39 ± 0.24
CYP3A4.10	18.17 ± 1.21 * ** ↓	47.63 ± 4.38 * ** ↓	0.38 ± 0.06
CYP3A4.11	136.61 ± 66.29	300.26 ± 186.92	0.52 ± 0.16
CYP3A4.14	41.46 ± 7.56	111.16 ± 49.64	0.40 ± 0.11
CYP3A4.15	90.53 ± 93.91	322.41 ± 418.85	0.42 ± 0.19
CYP3A4.16	36.84 ± 24.56	327.80 ± 394.48	0.18 ± 0.08
CYP3A4.17	2.71 ± 1.33 * ** ↓	410.30 ± 287.62	0.01 ± 0.00 * ** ↓
CYP3A4.18	50.27 ± 26.64	122.61 ± 104.80	0.49 ± 0.13
CYP3A4.19	66.68 ± 16.17	193.43 ± 70.15	0.36 ± 0.05
CYP3A4.23	186.80 ± 104.91	1024.63 ± 647.37	0.20 ± 0.03 * *↓
CYP3A4.24	ND	ND	ND
CYP3A4.28	28.32 ± 1.41 * ** ↓	204.80 ± 16.67 * ↑	0.14 ± 0.00 * ** ↓
CYP3A4.29	59.76 ± 1.54 * ↑	254.07 ± 30.99 * ↑	0.24 ± 0.03 * ↓
CYP3A4.31	23.20 ± 8.31 * ↓	82.31 ± 67.03	0.35 ± 0.13
CYP3A4.32	39.28 ± 3.84 * *↓	82.44 ± 7.16 * ** ↓	0.48 ± 0.03 * ** ↑
CYP3A4.33	29.05 ± 6.48 * *↓	78.47 ± 38.74 * ↓	0.40 ± 0.10
CYP3A4.34	28.23 ± 0.81 * ** ↓	63.33 ± 7.82 * ** ↓	0.45 ± 0.04 * *↑

Notes: Compared with CYP3A4.1, *P < 0.05, * *P < 0.01, * **P < 0.001. ND, not determined.

structures to PDBQT format. The human cytochrome P450 enzyme CYP3A4 (PDB ID: 4NZ2) was obtained from the RCSB Protein Data Bank database. AutodockTools 1.5.6 was also used to add polar hydrogen and charge to the CYP3A4 protein, which was subsequently converted to PDBQT format.

2.7. Statistic analysis

The data were presented as the mean ± standard deviation (SD). We used GraphPad Prism 9.5 software to create graphs showing the Michaelis-Menten curves, the half maximal inhibitory concentration (IC_{50}), and the mean plasma concentration-time. To calculate the pharmacokinetic parameters of ketamine and norketamine in rats using non-compartmental analysis, we used Drug and Statistics (DAS) software version 3.0. The significance of the parameters between the wild-type CYP3A4 and other variants was evaluated using the one-way analysis of variance (ANOVA) Dunnett test in SPSS version 20.0 (Chicago, IL, USA). Additionally, we compared the differences in pharmacokinetic parameters between two groups in rats using a t-test. $P < 0.05$ indicated statistically significant.

3. Results

3.1. Analytical method of UPLC-MS/MS

In present study, a strong linear relationship was observed between ketamine and norketamine within the concentration range of 0.05–1000 ng/ml. The calibration standard curves yielded the following linear regression equations: for ketamine, y = 0.0405948x + 0.661177 (R^2 = 0.9995); for norketamine, y = 0.0248701x + 0.0116341 (R^2 = 0.9991). The lower limit of quantification (LLOQ) for both ketamine and norketamine was determined to be 0.05 ng/ml. To assess the suitability of this bioanalytical method, we prepared quality control (QC) samples at low, medium, and high concentrations (n = 6). Accuracy, precision, stability, recovery, and matrix effects (ME) were evaluated as part of this assessment. Detailed results can be found in supplementary Tables S1-S3. .

3.2. Kinetic research of ketamine by recombinant human CYP3A4

Fig. 2 and Table 2 display the Michaelis-Menten curves and kinetic parameters of ketamine catalyzed by different variants of CYP3A4. Compared to wild-type CYP3A4, CYP3A4.5, .10, .17, .28, .31, .32, .33, .34 showed varying degrees of decrease in maximum reaction velocity

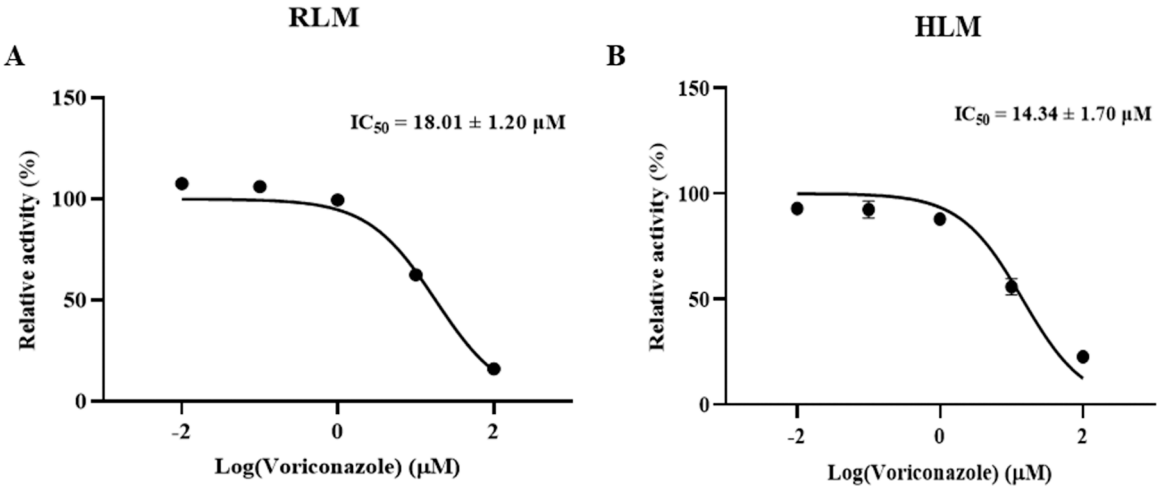

Fig. 3. Inhibition effect of voriconazole on ketamine metabolism. Half maximal inhibitory concentration (IC_{50}) of voriconazole (0.01, 0.1, 1, 10, and 100 μM) on the activity of rat liver microsomes (A) and human liver microsomes (B). Values are expressed as mean ± SD, n = 3. The data were fit to log (voriconazole concentration) vs. normalized response equations by GraphPad Prism 9.5.

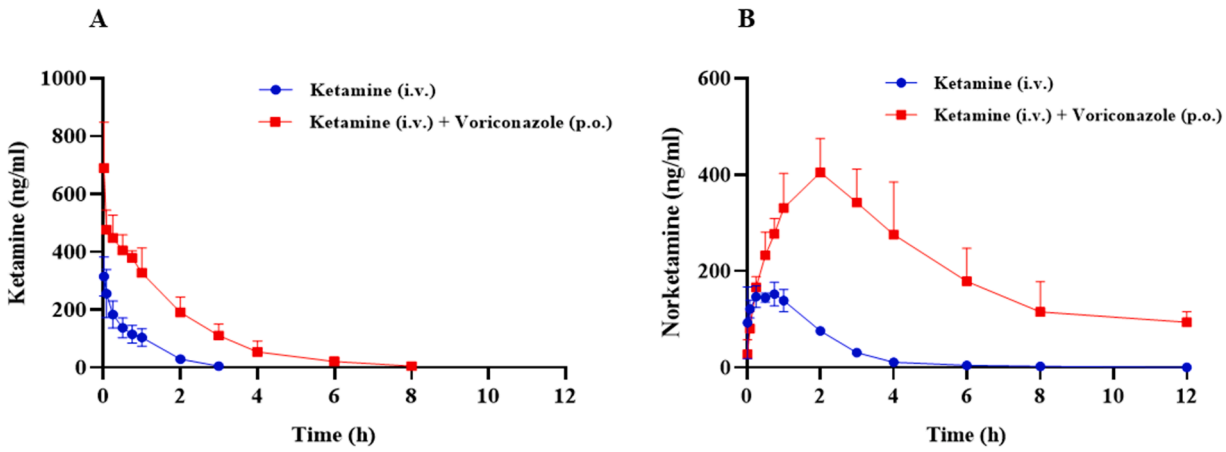

Fig. 4. Pharmacokinetic curves of ketamine with and without co-administration of voriconazole. The SD rats were subjected to animal experiment as indicated in the method. Mean plasma concentration-time curves of ketamine (A) and norketamine (B) in single group and combined group. Values are expressed as mean ± SD, n = 5.

Table 3
The main pharmacokinetic parameters of ketamine in two groups of rats (n = 5).

Parameters	Ketamine (i.v.)	Ketamine (i.v.) + voriconazole (p.o.)
$AUC_{(0-t)}$ (ng/L*h)	234.04 ± 66.57	998.07 ± 287.55 *
$AUC_{(0-\infty)}$ (ng/L*h)	247.85 ± 63.16	1019.93 ± 278.83 *
$t_{1/2z}$ (h)	0.52 ± 0.16	1.03 ± 0.35 *
$V_{z/F}$ (L/kg)	4.71 ± 1.85	2.20 ± 0.77 *
$CL_{z/F}$ (L/h/kg)	6.32 ± 1.32	1.56 ± 0.40 *
C_{max} (ng/ml)	314.24 ± 67.62	689.84 ± 158.08 *

Notes: AUC, area under the blood concentration–time curve; $t_{1/2z}$, elimination half time; T_{max}, peak time; $V_{z/F}$, apparent volume of distribution; $CL_{z/F}$, blood clearance; C_{max}, maximum blood concentration. *P < 0.05, compared with the control group.

Table 4
The main pharmacokinetic parameters of norketamine in two groups of rats (n = 5).

Parameters	Ketamine (i.v.)	Ketamine (i.v.) + Voriconazole (p.o.)
$AUC_{(0-t)}$ (ng/L*h)	348.90 ± 46.31	2311.46 ± 742.46 *
$AUC_{(0-\infty)}$ (ng/L*h)	350.04 ± 46.49	2659.72 ± 979.55 *
$t_{1/2z}$ (h)	1.80 ± 0.20	3.22 ± 1.15 *
$V_{z/F}$ (L/kg)	11.09 ± 2.07	2.64 ± 0.38 *
$CL_{z/F}$ (L/h/kg)	4.35 ± 0.58	0.63 ± 0.22 *
C_{max} (ng/ml)	162.46 ± 36.72	413.49 ± 68.44 *

Notes: AUC, area under the blood concentration–time curve; $t_{1/2z}$, elimination half time; T_{max}, peak time; $V_{z/F}$, apparent volume of distribution; $CL_{z/F}$, blood clearance; C_{max}, maximum blood concentration. *P < 0.05, compared with the control group.

(V_{max}) ranging from 26.68% to 94.94%. On the other hand, CYP3A4.29 showed an increase of 11.55% in V_{max}. In terms of Michaelis-Menten constant (K_m), variants CYP3A4.10, .32, .33, .34 exhibited a decrease from 169.60 ± 9.10 μM to 47.63 ± 4.38 μM, 82.44 ± 7.16 μM, 78.47 ± 38.74 μM, and 63.33 ± 7.82 μM, respectively. Meanwhile, CYP3A4.28 and CYP3A4.29 showed an increase of 1.2–1.5-fold compared to CYP3A4.1. Changes in V_{max} and K_m values of CYP3A4 mutants impact the clearance (CL_{int}) of the enzyme, which is commonly used as a standard for evaluating its activity. Compared to CYP3A4.1, significant increases (40.63%−87.50%) were observed in CYP3A4.2, .32, and .34, while significant decreases (25.00%−96.88%) were observed in CYP3A4.5, .17, .23, .28, and .29.

3.3. Inhibition of ketamine metabolism by voriconazole in vitro and in vivo

In the in vitro experiment, it was found that voriconazole inhibited more than 75% of ketamine metabolism. Fig. 3 displayed the IC_{50} values of voriconazole on ketamine metabolism, with RLM and HLM having values of 18.01 ± 1.20 μM and 14.34 ± 1.70 μM, respectively. These values were not significantly different from each other.

In the in vivo study, the main pharmacokinetic parameters of ketamine and norketamine were significantly altered in single group and combined group. Fig. 4 illustrated the area under the concentration-time curve (AUC) of ketamine and norketamine. Tables 3 and 4 provided the pharmacokinetic parameters of the two groups. Compared with ketamine alone, co-administrated of voriconazole exhibited a notable increase in C_{max} for both ketamine and norketamine, along with an increase in AUC. The C_{max} of ketamine was doubled, while the C_{max} of norketamine was quadrupled. Similarly, the AUC of ketamine was quadrupled, while the AUC of norketamine was tripled. The prolongation of $t_{1/2Z}$ was attributed to the decrease in $V_{z/F}$ and $CL_{z/F}$ for both ketamine and norketamine.

3.4. Molecular docking of ketamine and voriconazole with CYP3A4

Ketamine and voriconazole were both docked to the active pocket of CYP3A4, with respective affinities of − 6.9 kcal/mol and − 7.7 kcal/mol. In Fig. 5, it can be observed that the ketamine molecule occupies a hydrophobic cavity formed by the amino acid residues ILE-301, PHE-304, ALA-305, ILE-369, and ALA-370, forming a stable hydrophobic interaction. Further analysis revealed that the phenyl group of ketamine can undergo π-π stacking with HEM-1500. These interactions contribute to the formation of a stable complex between ketamine and CYP3A4. Similarly, the 2,4-difluorophenyl group of voriconazole occupies a hydrophobic cavity formed by the same amino acid residues mentioned earlier, also resulting in a stable hydrophobic interaction. Additionally, the voriconazole pyrimidine ring can form a cation-π interaction with the side chain of the amino acid residue ARG-105, while the 2,4-difluorophenyl group can form an anion-π interaction with the side chain of the amino acid residue GLU-308. Importantly, the voriconazole triazole ring can also undergo π-π stacking with HEM-1500. Therefore, when ketamine and voriconazole are used together, they may compete for the same binding site and spatial location.

4. Discussion

Ketamine is widely used in clinical settings, but its anesthetic and

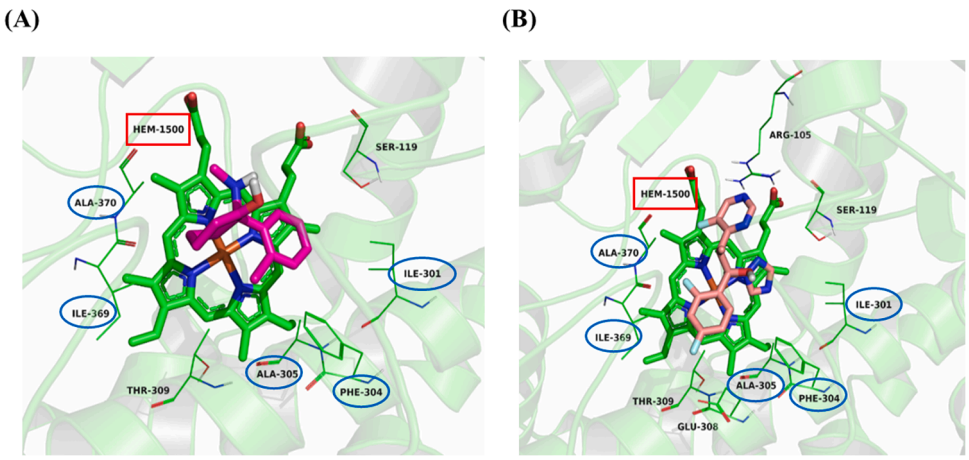

Fig. 5. Molecular docking of ketamine and voriconazole with CYP3A4. Ketamine and CYP3A4 molecular docking analysis (A), voriconazole and CYP3A4 molecular docking analysis (B).

central nerve reinforcing properties have led to widespread abuse (Liu et al. 2016). The clinical efficacy and individual variability in toxicity are also commonly observed with this drug. From a pharmacokinetic perspective, it is metabolized into norketamine by enzymes CYP3A4 and CYP2C9. Due to the genetic polymorphism of CYP enzymes, there may be individual differences in their metabolism, which can result in stratification of clinical efficacy. Indeed, our team has previously elucidated the pharmacokinetic characteristics of ketamine metabolism by the CYP2C9 enzyme (Zheng et al. 2017). Furthermore, there were notable interindividual differences in the enzyme activity of CYP3A4 variants towards substrates (Cai et al. 2021; Gao et al. 2022; Xu et al. 2023). In this study, we made the discovery that the presence of CYP3A4.2 (S222P) resulted in an 87.50% increase in ketamine metabolism. However, it was observed to have a limited impact on lidocaine metabolism in vitro, with a relatively modest change in the clearance rate (CL_{int}) of 27.93% compared to the wild-type (Fang et al. 2017).

The discrepancy in enzyme activity observed between the two substrates may be attributed to variations in the binding sites of the enzyme and substrates. It is plausible that the substitution of serine with proline at codon 222 in CYP3A4.2 increased the exposure of the ketamine binding site to the enzyme, compared to lidocaine. In contrast, CYP3A4.17 (F189S) exhibited a diminished ability to bind with ketamine, resulting in a lower affinity. This reduced affinity was similar to the alterations observed in the metabolic capacity of chlorpyrifos and testosterone (Dai et al. 2001). Notably, norketamine was not detected during the in vitro incubation of CYP3A4.24. *CYP3A4 * 24* might lead to a reduction in enzyme activity or a modification in the enzyme's binding site for ketamine, ultimately resulting in a weakened metabolic capacity.

With the advancement of modern medicine, the practice of combining different drugs has become increasingly common. One of the key mechanisms behind drug-drug interactions, which are influenced by the way drugs are processed in the body, is the inhibition of CYP450. This mechanism often occurs when two drugs compete for the same binding site on the enzyme (Manikandan and Nagini, 2018). Research has indicated that the combination of ketamine and clarithromycin, a potent CYP3A4 inhibitor, resulted in a significant increase in the mean $AUC_{(0-\infty)}$ of ketamine by 2.6 times and the average C_{max} of ketamine by 3.6 times (Hagelberg et al. 2010). We have chosen to investigate the effect of voriconazole, a potent inhibitor of CYP3A4, on the metabolism of ketamine. Our in vitro results showed that voriconazole strongly inhibited the production of norketamine, with IC_{50} of 18.01 ± 1.20 μM in RLM and 14.34 ± 1.70 μM in HLM. In vivo studies, we found that the combination of voriconazole and ketamine significantly increased the C_{max}, AUC, and $t_{1/2Z}$ of ketamine compared to the single administration of ketamine. With a limitation in mind, we made a deliberate decision to exclusively include male Sprague-Dawley rats in our study. This choice was driven by the fact that female rats undergo an estrous cycle, which involves hormonal fluctuations, particularly in estrogen and progesterone levels. These hormonal changes can have a notable influence on drug metabolism and introduce variability in experimental outcomes. Nevertheless, it is crucial to acknowledge that extrapolating the findings from male rats to the female population may have its constraints. Therefore, it is advisable to exercise caution when applying the results of this study to female subjects.

Molecular docking results revealed that both ketamine and voriconazole have a similar affinity for the active pocket of CYP3A4 and can form stable complexes with the enzyme. Additionally, voriconazole is also metabolized by CYP3A4 (Murayama et al. 2007). Therefore, it is possible that these two drugs compete for the same binding sites to inhibit the N-demethylation of ketamine. However, the transformation trend of norketamine was consistent with that of ketamine, although its pharmacological activity was only approximately 20% of ketamine (Leung and Baillie, 1986). In secondary metabolism, norketamine will be metabolized to an inactive hydroxynorketamine through CYP2B6 and CYP2A6 (Portmann et al. 2010). Voriconazole inhibited CYP3A4, it also was a strong suppressant of CYP2B6 ($K_i < 0.5$) (Jeong et al. 2009). Therefore, voriconazole increased blood exposure to norketamine, probably by inhibiting the enzymatic activity of CYP2B6.

Although ketamine has pharmacological benefits such as anesthesia, analgesia, and antidepressant effects, it is also associated with dissociative, psychotomimetic, cognitive, and peripheral side effects (Zanos et al. 2018). In this study, we identified several weakly metabolized alleles (*CYP3A4 *5*, **17*, **23*, **28*, and **29*) among the 22 CYP3A4 variants. Individuals carrying these alleles should exercise caution and adjust dosages to prevent hallucinations, drug dependence, and potential genotoxicity resulting from excessive ketamine concentrations. Conversely, there were three strong metabolic alleles (*CYP3A4 *2*, **32*, and **34*), which indicate that patients with high metabolic capacity may require special attention to ensure optimal drug treatment. Furthermore, the co-administration of ketamine and voriconazole can potentially enhance the pharmacological effects and even toxicity of ketamine, highlighting the importance for healthcare providers to exercise caution when using these two drugs together.

5. Conclusions

CYP3A4 gene polymorphism and the inhibitory effect of voriconazole can impact the metabolism of ketamine, leading to fluctuations in blood-drug levels. Consequently, in clinical practice, it is crucial to consider both the genotype of the CYP3A4 gene and potential drug interactions, with particular attention to CYP3A4 inhibitors.

Declaration of Competing Interest

The authors declare that they have no known competing financial interests or personal relationships that could have appeared to influence the work reported in this paper.

Data availability

Data will be made available on request.

Acknowledgments and Funding

This work was supported by the National Key Research and Development Program of China (2020YFC2008301), the National Natural Science Foundation of China (81973397), the Natural Science Foundation of Zhejiang Province (LTGC23H310001). We thank the Scientific Research Center of Wenzhou Medical University for their consultation and for providing us with the use of their instruments to support this work.

Appendix A. Supporting information

Supplementary data associated with this article can be found in the online version at doi:10.1016/j.tox.2023.153682.

References

Almazroo, O.A., Miah, M.K., Venkataramanan, R., 2017. Drug metabolism in the liver. Clin. Liver Dis. 21, 1–20.
Cai, Y., Lin, Q., Jin, Z., Xia, F., Ye, Y., Xia, Y., Papadimos, T.J., Wang, Q., Hu, G., Cai, J., Chen, L., 2021. Evaluation of recombinant CYP3A4 variants on the metabolism of oxycodone in vitro. Chem. Res. Toxicol. 34, 103–109.
Cheng, P.S., Fu, C.Y., Lee, C.H., Liu, C., Chien, C.S., 2007. GC-MS quantification of ketamine, norketamine, and dehydronorketamine in urine specimens and comparative study using ELISA as the preliminary test methodology. J. Chromatogr. B Anal. Technol. Biomed. Life Sci. 852, 443–449.
Culp, C., Kim, H.K., Abdi, S., 2020. Ketamine use for cancer and chronic pain management. Front Pharm. 11, 599721.
Dai, D., Tang, J., Rose, R., Hodgson, E., Bienstock, R.J., Mohrenweiser, H.W., Goldstein, J.A., 2001. Identification of variants of CYP3A4 and characterization of their abilities to metabolize testosterone and chlorpyrifos. J. Pharm. Exp. Ther. 299, 825–831.
Desta, Z., Moaddel, R., Ogburn, E.T., Xu, C., Ramamoorthy, A., Venkata, S.L., Sanghvi, M., Goldberg, M.E., Torjman, M.C., Wainer, I.W., 2012. Stereoselective and regiospecific hydroxylation of ketamine and norketamine. Xenobiotica 42, 1076–1087.
Dong, T.T., Mellin-Olsen, J., Gelb, A.W., 2015. Ketamine: a growing global health-care need. Br. J. Anaesth. 115, 491–493.
Fang, P., Tang, P.F., Xu, R.A., Zheng, X., Wen, J., Bao, S.S., Cai, J.P., Hu, G.X., 2017. Functional assessment of CYP3A4 allelic variants on lidocaine metabolism in vitro. Drug Des. Devel Ther. 11, 3503–3510.
Gao, N., Zhang, X., Hu, X., Kong, Q., Cai, J., Hu, G., Qian, J., 2022. The Influence of CYP3A4 Genetic Polymorphism and Proton Pump Inhibitors on Osimertinib Metabolism. Front Pharm. 13, 794931.
Gorlin, A.W., Rosenfeld, D.M., Ramakrishna, H., 2016. Intravenous sub-anesthetic ketamine for perioperative analgesia. J. Anaesthesiol. Clin. Pharm. 32, 160–167.
Guengerich, F.P., Waterman, M.R., Egli, M., 2016. Recent structural insights into cytochrome P450 function. Trends Pharm. Sci. 37, 625–640.
Hagelberg, N.M., Peltoniemi, M.A., Saari, T.I., Kurkinen, K.J., Laine, K., Neuvonen, P.J., Olkkola, K.T., 2010. Clarithromycin, a potent inhibitor of CYP3A, greatly increases exposure to oral S-ketamine. Eur. J. Pain. 14, 625–629.
Hashimoto, K., 2009. Emerging role of glutamate in the pathophysiology of major depressive disorder. Brain Res Rev. 61, 105–123.
Hijazi, Y., Boulieu, R., 2002. Contribution of CYP3A4, CYP2B6, and CYP2C9 isoforms to N-demethylation of ketamine in human liver microsomes. Drug Metab. Dispos. 30, 853–858.
Jeong, S., Nguyen, P.D., Desta, Z., 2009. Comprehensive in vitro analysis of voriconazole inhibition of eight cytochrome P450 (CYP) enzymes: major effect on CYPs 2B6, 2C9, 2C19, and 3A. Antimicrob. Agents Chemother. 53, 541–551.
Lelievre, B., Briet, M., Godon, C., Legras, P., Riou, J., Vandeputte, P., Diquet, B., Bouchara, J.P., 2018. Impact of infection status and cyclosporine on voriconazole pharmacokinetics in an experimental model of cerebral scedosporiosis. J. Pharm. Exp. Ther. 365, 408–412.
Leung, L.Y., Baillie, T.A., 1986. Comparative pharmacology in the rat of ketamine and its two principal metabolites, norketamine and (*Z*)-6-hydroxynorketamine. J. Med Chem. 29, 2396–2399.
Licata, M., Pierini, G., Popoli, G., 1994. A fatal ketamine poisoning. J. Forensic Sci. 39, 1314–1320.
Liu, Y., Lin, D., Wu, B., Zhou, W., 2016. Ketamine abuse potential and use disorder. Brain Res. Bull. 126, 68–73.
Manikandan, P., Nagini, S., 2018. Cytochrome P450 structure, function and clinical significance: a review. Curr. Drug Targets 19, 38–54.
Murayama, N., Imai, N., Nakane, T., Shimizu, M., Yamazaki, H., 2007. Roles of CYP3A4 and CYP2C19 in methyl hydroxylated and N-oxidized metabolite formation from voriconazole, a new anti-fungal agent, in human liver microsomes. Biochem Pharm. 73, 2020–2026.
Nicolas, J.M., Espie, P., Molimard, M., 2009. Gender and interindividual variability in pharmacokinetics. Drug Metab. Rev. 41, 408–421.
Noppers, I., Olofsen, E., Niesters, M., Aarts, L., Mooren, R., Dahan, A., Kharasch, E., Sarton, E., 2011. Effect of rifampicin on S-ketamine and S-norketamine plasma concentrations in healthy volunteers after intravenous S-ketamine administration. Anesthesiology 114, 1435–1445.
Percie du Sert, N., Ahluwalia, A., Alam, S., Avey, M.T., Baker, M., Browne, W.J., Clark, A., Cuthill, I.C., Dirnagl, U., Emerson, M., Garner, P., Holgate, S.T., Howells, D.W., Hurst, V., Karp, N.A., Lazic, S.E., Lidster, K., MacCallum, C.J., Macleod, M., Pearl, E.J., Petersen, O.H., Rawle, F., Reynolds, P., Rooney, K., Sena, E. S., Silberberg, S.D., Steckler, T., Wurbel, H., 2020. Reporting animal research: explanation and elaboration for the ARRIVE guidelines 2.0. PLoS Biol. 18, e3000411.
Portmann, S., Kwan, H.Y., Theurillat, R., Schmitz, A., Mevissen, M., Thormann, W., 2010. Enantioselective capillary electrophoresis for identification and characterization of human cytochrome P450 enzymes which metabolize ketamine and norketamine in vitro. J. Chromatogr. A 1217, 7942–7948.
Reus, G.Z., Simoes, L.R., Colpo, G.D., Scaini, G., Oses, J.P., Generoso, J.S., Prossin, A.R., Kaddurah-Daouk, R., Quevedo, J., Barichello, T., 2017. Ketamine potentiates oxidative stress and influences behavior and inflammation in response to lipolysaccharide (LPS) exposure in early life. Neuroscience 353, 17–25.
Roco, A., Quinones, L., Agundez, J.A., Garcia-Martin, E., Squicciarini, V., Miranda, C., Garay, J., Farfan, N., Saavedra, I., Caceres, D., Ibarra, C., Varela, N., 2012. Frequencies of 23 functionally significant variant alleles related with metabolism of antineoplastic drugs in the chilean population: comparison with caucasian and asian populations. Front Genet 3, 229.
Sleigh, J., Pullon, R.M., Vlisides, P.E., Warnaby, C.E., 2019. Electroencephalographic slow wave dynamics and loss of behavioural responsiveness induced by ketamine in human volunteers. Br. J. Anaesth. 123, 592–600.
Spurr, N.K., Gough, A.C., Stevenson, K., Wolf, C.R., 1989. The human cytochrome P450 CYP3 locus: assignment to chromosome 7q22-qter. Hum. Genet 81, 171–174.
Werk, A.N., Cascorbi, I., 2014. Functional gene variants of CYP3A4. Clin. Pharm. Ther. 96, 340–348.
Xu, R.A., Li, Q.Q., Gao, N.Y., Wang, J., Li, X.Y., Ye, F., Ni, J.H., Hu, G.X., Qian, J.C., 2023. Effect of flavonoids and CYP3A4 variants on midostaurin metabolism. Food Chem. Toxicol. 174, 113669.
Zanos, P., Moaddel, R., Morris, P.J., Riggs, L.M., Highland, J.N., Georgiou, P., Pereira, E. F.R., Albuquerque, E.X., Thomas, C.J., Zarate Jr., C.A., Gould, T.D., 2018. Ketamine and ketamine metabolite pharmacology: insights into therapeutic mechanisms. Pharm. Rev. 70, 621–660.
Zheng, X., Fang, P., Bao, S.S., Lin, D., Cai, J.P., Hu, G.X., 2017. Function of 38 variants CYP2C9 polymorphism on ketamine metabolism in vitro. J. Pharm. Sci. 135, 8–13.